

UC Berkeley

UC Berkeley Previously Published Works

Title

Investigation of Indigoidine Synthetase Reveals a Conserved Active-Site Base Residue of Nonribosomal Peptide Synthetase Oxidases

Permalink

<https://escholarship.org/uc/item/5km8x4kd>

Journal

Journal of the American Chemical Society, 142(25)

ISSN

0002-7863

Authors

Pang, Bo

Chen, Yan

Gan, Fei

et al.

Publication Date

2020-06-24

DOI

10.1021/jacs.0c04328

Peer reviewed

# Investigation of Indigoidine Synthetase Reveals Conserved Active Site Base Residue of Nonribosomal Peptide Synthetase Oxidases

Bo Pang<sup>†,‡,§</sup>, Yan Chen<sup>‡,§</sup>, Fei Gan<sup>†,‡,§</sup>, Chunsheng Yan<sup>‡</sup>, Liyuan Jin<sup>‡</sup>, Jennifer W. Gin<sup>‡,§</sup>, Christopher J. Petzold<sup>‡,§</sup>, Jay D. Keasling<sup>\*,†,‡,§,¶,#,○</sup>

<sup>†</sup>QB3 Institute, University of California, Berkeley, Berkeley, California 94720, United States

<sup>‡</sup>Joint BioEnergy Institute, Emeryville, California 94608, United States

<sup>§</sup>Biological Systems and Engineering Division, Lawrence Berkeley National Laboratory, Berkeley, California 94720, United States

<sup>¶</sup>Department of Chemical & Biomolecular Engineering, Department of Bioengineering, University of California, Berkeley, Berkeley, California 94720, United States

<sup>#</sup>Novo Nordisk Foundation Center for Biosustainability, Technical University Denmark, DK2970 Horsholm, Denmark

<sup>○</sup>Center for Synthetic Biochemistry, Shenzhen Institutes for Advanced Technologies, Shenzhen 518055, P. R. China

**ABSTRACT:** Nonribosomal peptide synthetase (NRPS) oxidase (Ox) domains oxidize protein-bound intermediates to install crucial structural motifs in bioactive natural products. The mechanism of this domain remains elusive. Here, by studying indigoidine synthetase, a single-module NRPS involved in the biosynthesis of indigoidine and several other bacterial secondary metabolites, we demonstrate that its Ox domain utilizes an active site base residue, tyrosine 665, to deprotonate protein-bound L-glutamyl residue. We further validate the generality of this active site residue among NRPS Ox domains. These findings not only resolve the biosynthetic pathway mediated by indigoidine synthetase but enable mechanistic insight into NRPS Ox domains.

Nonribosomal peptide synthetases (NRPSs) and some polyketide synthases (PKSs) are modular enzymes employing a thio-template mechanism to synthesize secondary metabolites. Compared to other template mechanisms, including those in polynucleotide and polypeptide synthesis, the thio-template mechanism features intensive modifications in the linear extension stage, leading to more diversified structures in the product portfolio.<sup>1,2</sup> The NRPS oxidase (Ox) domain usually oxidizes thiazoline, derived from L-cysteine by the cyclization (Cy) domain, to thiazole on the growing intermediate.<sup>3–6</sup> The resulting thiazole often plays a key role in the bioactivity of related thio-template products such as the anti-cancer agents epothilone and bleomycin and the toxin colibactin (**Figure 1a**).<sup>7–9</sup> However, the lack of a mechanistic understanding of the NRPS Ox domains, especially for the defining biochemical active site residue, has hindered its engineering.<sup>10</sup>

Indigoidine synthetase is an excellent model to study the catalytic mechanism of NRPS Ox domains because of its simple domain organization. Indigoidine synthetases are single-module NRPSs that have an Ox domain embedded in the N-terminal adenylation (A) domain, followed by a peptidyl carrier protein (PCP) domain, and a thioesterase (TE) domain (**Figure 1b**).<sup>11,12</sup> These NRPSs having a 4'-phosphopantetheine (Ppant) modification on the PCP domain (*holo* form) convert L-glutamine to 5-amino-3*H*-pyridine-2,6-dione (**1**), a putative product that is readily oxidized to a 3,3'-bipyridyl natural product, indigoidine (**2**), which as a bright blue color.<sup>12–15</sup> Indigoidine synthetase genes have been engineered and introduced into living systems to construct a cross-kingdom reporter system<sup>16</sup>, generate blue

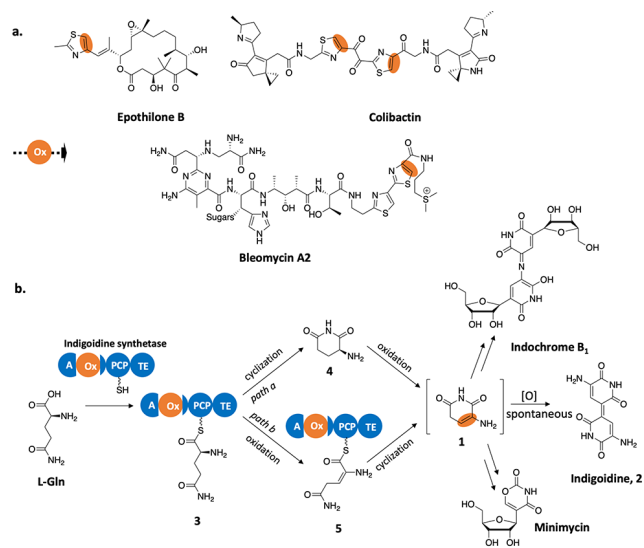


**Figure 1.** NRPS oxidase (Ox) domain in natural product biosynthesis. (a) Selected natural products containing the double bond (highlighted in yellow) installed by the NRPS Ox domain (b) Proposed biosynthesis pathways mediated by indigoidine synthetase to produce 5-amino-3*H*-pyridine-2,6-dione (**1**), a precursor for diverse compounds. *Paths a* (cyclization first followed by oxidation) and *b* (oxidation first followed by cyclization) are indicated in the figure.

rose<sup>17</sup>, and produce **2** as a promising water-insoluble dye<sup>18,19</sup>. Interestingly, indigoidine synthetase genes are widely distributed in bacteria, including *Actinobacteria* and *Proteobacteria* (Figure S1), and frequently colocalized with genes encoding enzymes that glycosylate C-5 of **1**, leading to the water-soluble blue pigment indochrome<sup>20,21</sup>, and the C-nucleoside antibiotic, minimycin<sup>13</sup> (Figure 1b). As such, indigoidine synthetases are involved in biosynthesis of a broad range of bacterial secondary metabolites. Nevertheless, how indigoidine synthetases catalyze the formation of **1** is not fully elucidated. Studies have validated that the A domain selectively activates and loads L-glutamine to afford L-glutaminyl-S-PCP (**3**), and the flavin mononucleotide (FMN) cofactor bound in the Ox domain is essential for indigoidine synthetases' activity.<sup>11</sup> The conversion of **3** to **1** by indigoidine synthetase is a black box (Figure 1b): **3** can be either first cyclized by the TE domain to  $\alpha$ -amino glutarimide (**4**) and then oxidized by the Ox domain to form **1** (*path a*),<sup>11,12</sup> or **3** can be first oxidized to dehydroglutaminyl-S-PCP (**5**) and then cyclized to **1** (*path b*).<sup>13</sup> Here, by monitoring the acylation changes on the PCP domain, we resolved the biosynthesis by indigoidine synthetase, which reveals the catalytic mechanism of NRPS Ox domains.

To establish a suitable system for this study, we chose BpsA, the indigoidine synthetase from *Streptomyces lavendulae*, which is readily expressed in several hosts, and reconstituted its activity *in vitro* based on previous studies.<sup>11,19,22</sup> *holo*-BpsA was purified from *Escherichia coli* BAP1<sup>23</sup> (Figure S2) and then incubated with L-glutamine in the presence of ATP and MgCl<sub>2</sub>. As expected, high-performance liquid chromatography (HPLC)

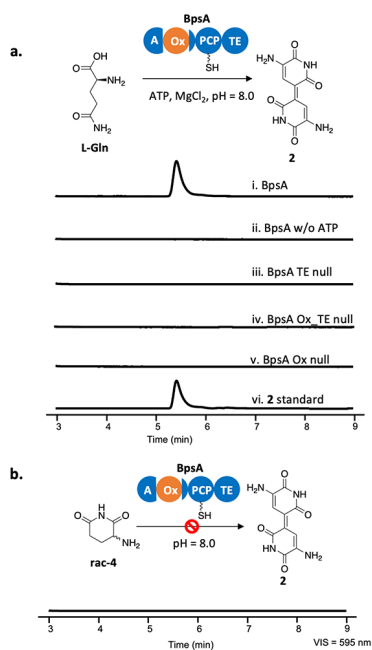


**Figure 2.** HPLC-DAD to determine indigoidine production. (a) *in vitro* assay of BpsA wild type and mutants using L-glutamine as substrate. The *in vitro* assay was conducted using *holo*-BpsA (i) and its domain inactive mutants: TE inactive (iii), Ox and TE inactive (iv), and Ox inactive (v). The assay using *holo*-BpsA without ATP addition was conducted as the negative control (ii). Chemically synthesized indigoidine was used as standard (vi). (b) Hypothesized *path a* (see Figure 1) test using racemic **4**.

analysis indicated the production of **2**, confirmed with a synthesized standard, while the negative control without ATP does not produce **2**. (Figure 2a-i, ii, vi).

We next tested the hypothesized *path a* (Figure 1b) by incubating **4** with BpsA: if the reaction proceeds via *path a*, the Ox domain would oxidize **4** into **1**, and then afford **2**, which can be readily detected by HPLC. Hence, we incubated *holo*-BpsA with racemic **4**, a commercially available reagent. HPLC analysis of the reaction mixture indicated no **2** production (Figure 2b), suggesting that *path a* may not be the pathway to produce **1**.

We then tested *path b* by monitoring the acylation change on the PCP active site Ser residue via a shotgun proteomics method, in which the protein is trypsinized to generate liquid chromatography tandem mass spectrometry (LC-MS/MS) detectable peptides. First, from the trypsinized *holo*-BpsA peptide mixture, we mapped a peptide, ENASVQDDFFESGGNS<sub>972</sub>(Ppant)LIAVGLVR, that contains the PCP domain active site residue (S972) with Ppant modification using proteomics search engine.<sup>24</sup> The extracted ion chromatogram (EIC) of its ion ( $m/z=955.4440$ ,  $[M+3H]^{3+}$ ) exhibited a single peak at a retention time of 29.2 min (Figure S3a). The MS isotopic profile and tandem MS fragmentation by collision-induced dissociation (CID) are consistent with the theoretical patterns for the peptide containing the PCP active site residue (Figure S3b,c). Notably, we observed the Ppant ejection ion, a signature fragment ion of Ppant generated from CID, in tandem MS analysis (Figure S3d).<sup>25,26</sup> Because the Ppant is acylated in thiotemplate biosynthesis, any changes in acylation can be tracked by monitoring changes in the molecular weight corresponding to the ejected Ppant ions from the PCP derived peptides, which can be first identified by the unchanged peptide fragment ions.

To detect acylation changes on the PCP domain in the biosynthesis, we next followed the BpsA *in vitro* reconstitution reaction by LC-MS/MS analysis. However, we could not detect any acylation changes on the mapped peptide. Since BpsA efficiently converts L-glutamine,<sup>27</sup> we reasoned that the amount of intermediates on the PCP might be below the detection limit of the assay. To accumulate possible intermediates on the PCP, we inactivated the TE domain by site-directed mutagenesis (Figure S4). The resulting mutant (BpsA S1102A, TE null, Figure S2) loses the ability to produce **2** *in vitro* (Figure 2a-iii). Upon analyzing the acylation changes on the PCP domain, we failed to detect the ion corresponding to the peptide from **5** ( $m/z=997.4583$ ,  $[M+3H]^{3+}$ ). Instead, we observed a new PCP-derived peptide ion ( $m/z=997.7863$ ,  $[M+3H]^{3+}$ ) that has +1 Da mass shift from **5** (Figure 3b-ii and S5). Inspired by the reaction catalyzed by amino acid oxidases,<sup>28</sup> we hypothesized that the new product is 5-amino-2,5-dioxopentyl-S-PCP (**6**), the hydrolyzed product of **5** (Figure 3a). To confirm the hydrolysis, we substituted L-glutamine with L-[amino-<sup>15</sup>N]glutamine and L-[amide-<sup>15</sup>N]glutamine in the BpsA TE null assay. The results indicated that the <sup>15</sup>N isotope introduced into **6** from L-[amide-<sup>15</sup>N]glutamine but not from L-[amino-<sup>15</sup>N]glutamine, in which the <sup>15</sup>N labeled amino group was proposed to be hydrolyzed (Figure 3c and S6). These data validate that indigoidine synthetases use *path b*, which comprises the proposed oxidation of **3** to **5**.

The clarified pathway allowed us to focus on the oxidation reaction presumably catalyzed by the Ox domain. We then inactivated the Ox domain and analyzed PCP acylation changes

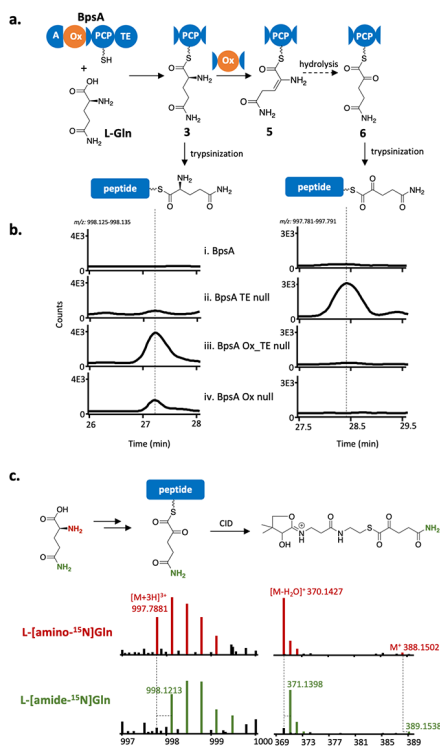


**Figure 3.** Assessing acylation changes on the BpsA PCP domain by LC-MS/MS. (a) The acylations on the PCP domain were analyzed via a shotgun proteomics method, in which the protein was trypsinized to yield MS detectable peptides. (b) Extracted ion chromatograms (EIC) of  $[M+3H]^{3+}$  peptide ions from L-glutaminylyl-S-PCP (**3**, left) and 5-amino-2,5-dioxopentyl-S-PCP (**6**, right) in the assay using BpsA or its mutants. (c) MS and tandem MS of the  $[M+3H]^{3+}$  peptide ions from 5-amino-2,5-dioxopentyl-S-PCP in the assay using L-[amino- $^{15}N$ ]glutamine (red) or L-[amide- $^{15}N$ ]glutamine (green).

of the resulting mutant. Given that changes in FMN binding residues of NRPS Ox domains generate FMN-free mutants,<sup>10,11</sup> we chose to target the active site residue of BpsA Ox domain for mutation to maintain overall structural integrity. Studies have suggested that NRPS Ox domains employ a base residue at the active site to deprotonate the  $C_{\alpha}$ -H of the PCP bound substrate to initial the oxidation reaction. However, the base residue has never been identified.<sup>3,29</sup> We then pursued to identify the base residue by attempting to resolve the structure of BpsA Ox domain. Although our initial attempts of crystallizing the truncated proteins were not successful, we were able to build a model of BpsA Ox domain using I-TASSER<sup>30</sup> with high confidence value (C-score = 0.79). A structural search of the PDB database using the BpsA Ox domain model identified five structures with TM-score above 0.8, in which McbC (PDB: 6GOS) came to our attention (**Table S3**) because its catalytic mechanism has been well studied.<sup>31</sup> McbC, a FMN-dependent dehydrogenase involved in the biosynthesis of the ribosomally synthesized and post-translationally modified peptide (RiPP) antibiotic microcin B17, oxidizes azoline to azole, a reaction resembling the ones catalyzed by most NRPS Ox domains. McbC and the NRPS Ox domain share some local amino acid sequence similarities, although their global amino acid identity is low (16.2%).<sup>4</sup> Taken

together, these results suggested that the BpsA Ox domain may employ a similar mechanism as McbC, which uses its Tyr202 as the base to abstract the  $\alpha$ -H of azoline (**Figure S8**). Alignment of the McbC structure with the model of BpsA Ox domain indicates that McbC Tyr202 overlaps with BpsA Tyr665, and that in both cases the Tyr side chain points to the FMN cofactor (**Figure 4a and S9**). These results allow us to hypothesize that BpsA Tyr665 is the active site base residue.

To test the hypothesized base residue, we changed Tyr665 to Phe in BpsA S1102A (TE null) mutant to remove the hydroxyl group, the proposed basic center. This mutant, BpsA Y665F S1102A (Ox\_TE null), keeps the FMN cofactor (**Figure S2**) but does not produce **2** *in vitro* (**Figure 2a-iv**). LC-MS/MS hardly detected the **6** derived peptide ions in the assay using the new mutant. Instead, **3**, the substrate of the Ox domain, accumulated (**Figure 3b-iii and S7**). We also assayed the mutant that has Y665F mutation in wild-type BpsA (BpsA Ox null), and got similar results (**Figure 3b-iv**). These data support our hypothesis that Tyr665 is the active site base residue of BpsA Ox domain.

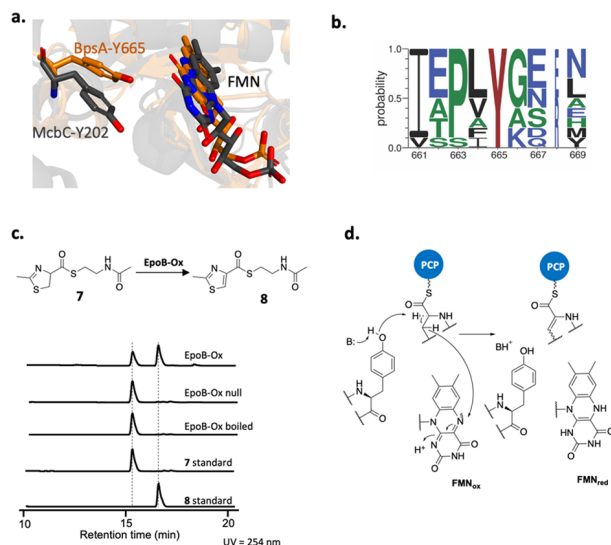


**Figure 4.** Mechanistic insight into NRPS Ox domains. (a) The active site key residue, Tyr 665, of BpsA Ox domain (yellow) was determined by structural alignment with McbC (gray), a RiPP dehydrogenase. The generality of the key Tyr residue was confirmed by (b) multiple sequence alignment of known NRPS Ox domains, and (c) biochemical assays of EpoB-Ox, the Ox domain in the PKS-NRPS assembly line for epothilone biosynthesis. (d) Proposed E2-like mechanism for NRPS Ox domains.

Next we explored the generality of Tyr as the active site base residue in NRPS Ox domains. The amino acid sequence alignment analysis indicates that the Tyr residue is conserved among all NRPS Ox domains (**Figure 4b and S10**). To validate the role of Tyr as active site residue in an alternative NRPS, we purified EpoB-Ox, the Ox domain of epothilone NRPS, from *E. coli* BL21(DE3) (**Figure S2**) and synthesized methylthiazolyl-S-acetylcysteamine (methylthiazolyl-S-NAC, **7**), a mimic for the PCP bound substrate of EpoB-Ox, as reported.<sup>3</sup> Incubating EpoB-Ox with **7** led to the expected product, methylthiazolyl-S-NAC (**8**) (**Figure 4c**). Changing EpoB-Ox Tyr162, the proposed active site base residue, to Phe resulted in a mutant (EpoB-Ox null) that retains FMN (**Figure S2**) but loses oxidative activity, a comparable result to boiled EpoB-Ox (**Figure**

**4c).** In light of the results of structural/sequence alignments and biochemical studies, we propose that NRPS oxidases share an McbC-like E2-elimination mechanism to catalyze the oxidation reactions: the tyrosine residue in the active site acts as the base to abstract the C $\alpha$ -H as a proton from the PCP bound substrate, whose C $\beta$ -H ejects as a hydride to N $_5$  of the bound FMN (**Figure 4d**). Considering the hydroxyl group of tyrosine is a weak base, we propose a coupled base residue, equivalent to Lys201 in McbC, polarizes the hydroxyl group to oxidize first. There is an adjacent Lys666 residue to Tyr665 in BpsA. However, it is not conserved in NRPS Ox domain amino acid sequences and poised oppositely to Tyr665 in the BpsA Ox domain model (**Figure S9b**). Research is in progress to address the detailed mechanism.

In summary, we resolved the specific biosynthetic pathway mediated by indigoidine synthetase, and further revealed the common mechanism of NRPS Ox domains. The revealed mechanism of NRPS Ox domains echo the unified paradigm of azoles biosynthesis in RiPPs and NRPS peptides.<sup>32</sup> Given that RiPPs biosynthesis also employs a template mechanism, these two different peptide natural product biosynthesis pathways use the same paradigm to install similar structural motifs in different biosynthesis stages.

## ASSOCIATED CONTENT

### Supporting Information

The Supporting Information is available free of charge on the ACS Publications website.

detailed methods, supplementary figures, supplementary tables, synthesized gene sequences  
PDB file of the BpsA Ox domain model

## AUTHOR INFORMATION

### Corresponding Author

\* Email: jdkeasling@lbl.gov

### Notes

J.D.K. has financial interests in Amyris, Lygos, Demetrix, Napigen, Maple Bio, Berkeley Brewing Sciences, Ansa Biotech and Apertor Labs.

## ACKNOWLEDGMENT

The authors thank Dr. Pablo Cruz-Morales for genome mining of indigoidine synthetase gene, and Drs. Maren Wehrs and Aindrila Mukhopadhyay for supplying plasmid for BpsA gene cloning. The authors also thank Drs. Leonard Katz, Jesus F. Barajas, and Yuzhong Liu for helpful discussions. This work was funded by the DOE Joint BioEnergy Institute (<http://www.jbei.org>) supported by the U.S. Department of Energy, Office of Science, Office of Biological and Environmental Research, through contract DE-AC02-05CH11231 between Lawrence Berkeley National Laboratory and the U.S. Department of Energy. Funds for the 900 MHz NMR spectrometer were provided by the NIH through grant GM68933.

## REFERENCES

(1) Pang, B.; Wang, M.; Liu, W. Cyclization of Polyketides and Non-Ribosomal Peptides on and off Their Assembly Lines. *Nat. Prod. Rep.* **2016**, *33*, 162–173.

- (2) Sundaram, S.; Hertweck, C. On-Line Enzymatic Tailoring of Polyketides and Peptides in Thiotemplate Systems. *Curr. Opin. Chem. Biol.* **2016**, *31*, 82–94.
- (3) Schneider, T. L.; Shen, B.; Walsh, C. T. Oxidase Domains in Epothilone and Bleomycin Biosynthesis: Thiazoline to Thiazole Oxidation during Chain Elongation. *Biochemistry* **2003**, *42*, 9722–9730.
- (4) Du, L.; Chen, M.; Sánchez, C.; Shen, B. An Oxidation Domain in the BlmIII Non-Ribosomal Peptide Synthetase Probably Catalyzing Thiazole Formation in the Biosynthesis of the Anti-Tumor Drug Bleomycin in *Streptomyces verticillus* ATCC15003. *FEMS Microbiol. Lett.* **2000**, *189*, 171–175.
- (5) Silakowski, B.; Schairer, H. U.; Ehret, H.; Kunze, B.; Weinig, S.; Nordsiek, G.; Brandt, P.; Blöcker, H.; Höfle, G.; Beyer, S.; Müller, R. New Lessons for Combinatorial Biosynthesis from Myxobacteria. The Myxothiazol Biosynthetic Gene Cluster of *Stigmatella aurantiaca* DW4/3-1. *J. Biol. Chem.* **1999**, *274*, 37391–37399.
- (6) Julien, B.; Shah, S.; Ziermann, R.; Goldman, R.; Katz, L.; Khosla, C. Isolation and Characterization of the Epothilone Biosynthetic Gene Cluster from *Sorangium cellulosum*. *Gene* **2000**, *249*, 153–160.
- (7) Nicolaou, K. C.; Roschangar, F.; Vourloumis, D. Chemical Biology of Epothilones. *Angew. Chem. Int. Ed.* **1998**, *37*, 2014–2045.
- (8) Hamamichi, N.; Natrajan, A.; Hecht, S. M. On the Role of Individual Bleomycin Thiazoles in Oxygen Activation and DNA Cleavage. *J. Am. Chem. Soc.* **1992**, *114*, 6278–6291.
- (9) Faïs, T.; Delmas, J.; Barnich, N.; Bonnet, R.; Dalmasso, G. Colibactin: More than a New Bacterial Toxin. *Toxins (Basel)* **2018**, *10*.
- (10) Trautman, E. P.; Healy, A. R.; Shine, E. E.; Herzon, S. B.; Crawford, J. M. Domain-Targeted Metabolomics Delineates the Heterocycle Assembly Steps of Colibactin Biosynthesis. *J. Am. Chem. Soc.* **2017**, *139*, 4195–4201.
- (11) Takahashi, H.; Kumagai, T.; Kitani, K.; Mori, M.; Matoba, Y.; Sugiyama, M. Cloning and Characterization of a *Streptomyces* Single Module Type Non-Ribosomal Peptide Synthetase Catalyzing a Blue Pigment Synthesis. *J. Biol. Chem.* **2007**, *282*, 9073–9081.
- (12) Reverchon, S.; Rouanet, C.; Expert, D.; Nasser, W. Characterization of Indigoidine Biosynthetic Genes in *Erwinia chrysanthemi* and Role of This Blue Pigment in Pathogenicity. *J. Bacteriol.* **2002**, *184*, 654–665.
- (13) Kong, L.; Xu, G.; Liu, X.; Wang, J.; Tang, Z.; Cai, Y.-S.; Shen, K.; Tao, W.; Zheng, Y.; Deng, Z.; Price, N. P. J.; Chen, W. Divergent Biosynthesis of C-Nucleoside Minimycin and Indigoidine in Bacteria. *iScience* **2019**, *22*, 430–440.
- (14) Kuhn, R.; Bauer, H.; Knackmuss, H.-J. Struktur Und Synthesen Des Bakterienfarbstoffs Indigoidin. *Chem. Ber.* **1965**, *98*, 2139–2153.
- (15) Knackmuss, H. J. Synthesis of 3-Amino-2,6-Pyridinediol. *J. Heterocycl. Chem.* **1970**, *7*, 733–734.
- (16) Müller, M.; Ausländer, S.; Ausländer, D.; Kemmer, C.; Fussenegger, M. A Novel Reporter System for Bacterial and Mammalian Cells Based on the Non-Ribosomal Peptide Indigoidine. *Metab. Eng.* **2012**, *14*, 325–335.
- (17) Nanjaraj Urs, A. N.; Hu, Y.; Li, P.; Yuchi, Z.; Chen, Y.; Zhang, Y. Cloning and Expression of a Nonribosomal Peptide Synthetase to Generate Blue Rose. *ACS Synth. Biol.* **2019**, *8*, 1698–1704.
- (18) Xu, F.; Gage, D.; Zhan, J. Efficient Production of Indigoidine in *Escherichia coli*. *J. Ind. Microbiol. Biotechnol.* **2015**, *42*, 1149–1155.
- (19) Wehrs, M.; Gladden, J. M.; Liu, Y.; Platz, L.; Prahl, J.-P.; Moon, J.; Papa, G.; Sundstrom, E.; Geiselman, G. M.; Tanjore, D.; Keasling, J. D.; Pray, T. R.; Simmons, B. A.; Mukhopadhyay, A. Sustainable Bioproduction of the Blue Pigment Indigoidine: Expanding the Range of Heterologous Products in *R. toruloides* to Include Non-Ribosomal Peptides. *Green Chem.* **2019**, *21*, 3394–3406.
- (20) Knackmuss, H. J.; Cosens, G.; Starr, M. P. The Soluble Blue Pigment, Indochrome, of *Arthrobacter polychromogenes*. *Eur. J. Biochem.* **1969**, *10*, 90–95.
- (21) Thapa, K.; Oja, T.; Metsä-Ketelä, M. Molecular Evolution of the Bacterial Pseudouridine-5'-Phosphate Glycosidase Protein Family. *FEBS J.* **2014**, *281*, 4439–4449.
- (22) Wehrs, M.; Prahl, J.-P.; Moon, J.; Li, Y.; Tanjore, D.; Keasling, J. D.; Pray, T.; Mukhopadhyay, A. Production Efficiency of the Bacterial Non-Ribosomal Peptide Indigoidine Relies on the Respiratory Metabolic State in *S. cerevisiae*. *Microb. Cell Fact.* **2018**, *17*, 193.

- (23) Pfeifer, B. A.; Admiraal, S. J.; Gramajo, H.; Cane, D. E.; Khosla, C. Biosynthesis of Complex Polyketides in a Metabolically Engineered Strain of *E. coli*. *Science* **2001**, *291*, 1790–1792.
- (24) Chi, H.; Liu, C.; Yang, H.; Zeng, W.-F.; Wu, L.; Zhou, W.-J.; Wang, R.-M.; Niu, X.-N.; Ding, Y.-H.; Zhang, Y.; Wang, Z.-W.; Chen, Z.-L.; Sun, R.-X.; Liu, T.; Tan, G.-M.; Dong, M.-Q.; Xu, P.; Zhang, P.-H.; He, S.-M. Comprehensive Identification of Peptides in Tandem Mass Spectra Using an Efficient Open Search Engine. *Nat. Biotechnol.* **2018**, *36*, 1059–1061.
- (25) Dorrestein, P. C.; Bumpus, S. B.; Calderone, C. T.; Garneau-Tsodikova, S.; Aron, Z. D.; Straight, P. D.; Kolter, R.; Walsh, C. T.; Kelleher, N. L. Facile Detection of Acyl and Peptidyl Intermediates on Thio-template Carrier Domains via Phosphopantetheinyl Elimination Reactions during Tandem Mass Spectrometry. *Biochemistry* **2006**, *45*, 12756–12766.
- (26) Blake-Hedges, J. M.; Pereira, J. H.; Cruz-Morales, P.; Thompson, M. G.; Barajas, J. F.; Chen, J.; Krishna, R. N.; Chan, L. J. G.; Nimlos, D.; Alonso-Martinez, C.; Baidoo, E. E. K.; Chen, Y.; Gin, J. W.; Katz, L.; Petzold, C. J.; Adams, P. D.; Keasling, J. D. Structural Mechanism of Regioselectivity in an Unusual Bacterial Acyl-CoA Dehydrogenase. *J. Am. Chem. Soc.* **2020**, *142*, 835–846.
- (27) Brown, A. S.; Robins, K. J.; Ackerley, D. F. A Sensitive Single-Enzyme Assay System Using the Non-Ribosomal Peptide Synthetase BpsA for Measurement of L-Glutamine in Biological Samples. *Sci. Rep.* **2017**, *7*, 41745.
- (28) Umhau, S.; Pollegioni, L.; Molla, G.; Diederichs, K.; Welte, W.; Pilone, M. S.; Ghisla, S. The X-Ray Structure of D-Amino Acid Oxidase at Very High Resolution Identifies the Chemical Mechanism of Flavin-Dependent Substrate Dehydrogenation. *Proc Natl Acad Sci USA* **2000**, *97*, 12463–12468.
- (29) Argueta, E. A.; Amoh, A. N.; Kafle, P.; Schneider, T. L. Unusual Non-Enzymatic Flavin Catalysis Enhances Understanding of Flavoenzymes. *FEBS Lett.* **2015**, *589*, 880–884.
- (30) Yang, J.; Yan, R.; Roy, A.; Xu, D.; Poisson, J.; Zhang, Y. The I-TASSER Suite: Protein Structure and Function Prediction. *Nat. Methods* **2015**, *12*, 7–8.
- (31) Ghilarov, D.; Stevenson, C. E. M.; Travin, D. Y.; Piskunova, J.; Serebryakova, M.; Maxwell, A.; Lawson, D. M.; Severinov, K. Architecture of Microcin B17 Synthetase: An Octameric Protein Complex Converting a Ribosomally Synthesized Peptide into a DNA Gyrase Poison. *Mol. Cell* **2019**, *73*, 749–762.e5.
- (32) Roy, R. S.; Gehring, A. M.; Milne, J. C.; Belshaw, P. J.; Walsh, C. T.; Roy, R. S.; Gehring, A. M.; Milne, J. C.; Belshaw, P. J.; Walsh, C. T. Thiazole and Oxazole Peptides: Biosynthesis and Molecular Machinery. *Nat. Prod. Rep.* **1999**, *16*, 249–263.

Insert Table of Contents artwork here

